Contents lists available at ScienceDirect

Journal of Luminescence

Phenothiazine derivatives as an easily accessible emitter for green light-emitting electrochemical cells

Kim Jongseong[a], Kanagaraj Shanmugasundaram[a], Ramesh Kumar Chitumalla[b], Joonkyung Jang[b], Youngson Choe[a],[*]

[a] School of Chemical and Biomolecular Engineering, Pusan National University, Busan 609-735, Republic of Korea
[b] Department of Nanoenergy Engineering, Pusan National University, Busan 609-735, Republic of Korea

ARTICLE INFO

ABSTRACT

A new phenothiazine derivatives of an ionic small molecules were synthesized and its photo- and electrochemical properties were evaluated. The compounds NPzN and PPzP exhibits good thermal stabilities and shows positive solvatochromism upon increasing the polarity of the solvents. The single-component electroluminescence devices were fabricated from solution by incorporating both the emitters. Light-emitting electrochemical cell devices exhibited green color electroluminescence for both the compounds with the CIE coordinates of (0.28, 0.43) and (0.32, 0.41). These results indicate that phenothiazine derivatives have a promising prospect in the application of solution processed green LECs.

1. Introduction

The use of organic molecules as light-emitter have received great interests in recent years. Organic materials offer promising structural modification to found their application in optoelectronic devices. The significant growth of organic light-emitting diodes (OLEDs) [1] have been reached commercialization through mobile phones, displays and televisions. The layers in the OLED devices were fabricated by high vacuum thermal evaporation technique. This technique leads to increase the device cost for bulk preparation of efficient OLED devices. The fabrication limitation of OLEDs stimulates the researcher to find the alternatives over OLEDs. Light-emitting electrochemical cells (LECs) [2–10] referred to as solid-state lighting devices having simpler device architecture than OLEDs. LECs are simple device structure and fabricated from solution under ambient condition for low-cost electroluminescent devices as compared to OLEDs. The first ever LEC was reported by Pei and coworkers in 1995 using the fluorescent polymer as the electroluminescent material mixed with an ionic transporting polymer and an inorganic salt were sandwiched between two metal electrodes. The electroluminescent materials in LECs are organic emitters either neutral conjugated polymer (CP) [11–17] or an ionic transition metal complex (iTMC) [18–22] enables both ionic and electronic conduction. In general, iTMC based LECs are derived from second- and third-row transition metal ions, due to their strong metal-ligand interaction and luminescent efficiencies [23–27]. Nowadays organic small molecules have been focused for developing high performance full-color flat panel displays and solid-state lighting technologies. Therefore, the synthesis of organic small molecules and establishment of their structural properties are essential for commercialization of cheaper products. The first organic small molecule based solid-state light emitting electrochemical cell was reported by Hill et al. [28]. The device architecture was similar to polymer based LEC devices. Thereafter, to simplify the thin film architecture, Chen et al. reported LEC devices based on an ionic terfluorene derivative as an active emitter [29]. An intrinsic ionic nature emerged great attention in LECs to develop charged organic small molecules for the ease of LEC fabrication. A solution processed LECs based organic small molecules have been effectively reported in recent years. Non-ionic [30–39] and ionic [40–50] small molecules are most commonly using active materials in LECs. The dual role of an ionic small molecules has attracted intensively to synthesize the fluorescent materials for LECs. In this study, we report an ionic phenothiazine based small molecules NPzN and PPzP comprising of naphthalene and phenanthrene cores. Both the compounds show green electroluminescence centered at 499 and 505 nm for compound NPzN and PPzP respectively, for the constructed LEC devices.

2. Experimental section

2.1. General information

^{1}H NMR spectra was measured with Varian unity Inova-300 MHz spectrometer at room temperature. Purification and spin coating

---

process were processed under an ambient condition. Differential scanning calorimetry (DSC) was performed using a TA instruments Q200 KBSI operated at a heating rate of $10\,°C\,min^{-1}$. The glass transition temperature (T_g) was determined from the second heating scan. Thermogravimetric analysis (TGA) was undertaken using a Netzsch TG 209 instrument. The thermal stability of the samples was determined by measuring their weight loss at a heating rate of $20\,°C\,min^{-1}$. The UV–visible absorption and photoluminescence spectra of the compound were recorded on a UV–VIS spectrometer, Lamda-20, PerkinElmer and Hitachi F-7000 FL spectrophotometer, respectively. Photoluminescence quantum yield (PLQY) was measured in toluene solution using 9, 10-diphenylanthracene as a standard. The optical band gap (E_g) was obtained from the absorption onset potential. Cyclic voltammetry (CV) measurements were performed on cyclic voltammetry (CV) model of potentiostat/galvanostat (Iviumstat) voltammetry analyzer with platinum as the working electrode, platinum wire as the counter electrode and Ag/AgCl as the reference electrode at a scanning rate $100\,mV\,s^{-1}$. Tetra-*n*-butylammonium hexafluoro phosphate (TBAPF$_6$, 0.10 M) was used as the supporting electrolyte and acetonitrile as the solvent, respectively. The experiments were calibrated with the standard ferrocenium/ferrocene (Fc$^+$/Fc) system. The HOMO energy level of the molecule calculated from the onset of oxidation potentials using the formula $E_{HOMO} = -4.40\text{-}E_{onset}$ (ox) and the LUMO was obtained by adding the E_g to the calculated HOMO energy level. All the reported quantum chemical calculations have been performed with Gaussian 09 program and for a computational simplicity, we have modeled the compounds NPzN and PPzP by removing the methyl group (on imidazole) and PF_6^- counter ion. First, the ground state structures of two compounds were optimized using the density functional theory (DFT). We used B3LYP [51–53] exchange-correlation functional in combination with 6-31G(d) basis set for optimization and frequency analysis. The optimized geometries were then subjected to the vibrational frequency analysis to confirm that the obtained configuration is indeed a minimum on the potential energy surface. The time dependent DFT (TDDFT) simulations were also performed on the optimized geometries to calculate the excitation energies. The TDDFT simulations were performed at the same [6-31G(d)] level of theory as used for the geometry optimization using CAM-B3LYP [54] functional which includes the long-range corrections. We model the experimental toluene solution using the polarizable continuum model (PCM) [55,56] in TDDFT simulations for correct description.

2.2. Synthesis

The active compounds NpzN and PPzP were designed and synthesized through multi-step reactions was depicted in Scheme 1. The intermediate compound 1 was synthesized according to previous report [48].

2.3. Synthesis of 2

Compound 1 (0.50 g, 0.96 mmol), 2-naphthalene boronic acid (0.41 g, 2.40 mmol), Pd(PPh$_3$)$_4$ (0.04 g, 0.04 mmol), TBAB (0.03 g, 0.10 mmol) and K$_2$CO$_3$ (0.66 g, 5.00 mmol) were added to 2:1 (V/V) mixture of tetrahydrofuran/water under argon atmosphere. The reaction mixture was refluxed at 70 °C for 24 h. Upon completion of the reaction, the mass was cooled to room temperature, the mixture was extracted with dichloromethane and dried over sodium sulfate. The extracted mass was concentrated under reduced pressure and the residue was purified by column chromatography on silica gel eluted with n-hexane/ethyl acetate (9/1; v/v) to afford compound 2 as solid. Yield: 76%. ^{1}H NMR (300 MHz, CDCl$_3$, δ): 7.94–7.82 (m, 4H), 7.78–7.66 (m, 4H), 7.60–7.36 (m, 10H), 7.16–7.06 (m, 2H), 3.80 (t, 2H), 3.45 (t, 2H), 2.10–1.90 (m, 4H), 1.75–1.50 (m, 4H).

2.4. Synthesis of 3

Using above synthetic procedure compound 3 was obtained as a solid by replacing 9-phenanthrene boronic acid instead of 2-naphthalene boronic acid. Yield: 79%. ^{1}H NMR (300 MHz, CDCl$_3$, δ): 7.93–7.78 (m, 6H), 7.70–7.58 (m, 10H), 7.45–7.35 (m, 4H), 7.25–7.20 (m, 4H), 3.83 (t, 2H), 3.40 (t, 2H), 2.15–1.96 (m, 4H), 1.79–1.52 (m, 4H).

2.5. Synthesis of NPzN

To the solution of compound 2 (0.25 g, 0.41 mmol) in 5 mL toluene was added excess 1-methylimidazole (2 mL) and the resulting reaction mixture was refluxed for overnight under argon atmosphere. After completion of reaction, the reaction mass was concentrated and the final product NPzN was obtained by adding saturated NH$_4$PF$_6$ solution and stirred for 2 h. Then the resulting solid was filtered and washed several times with water and hexane. The product was dried in vacuum at 45 °C for 16 h. Yield: 72%. ^{1}H NMR (300 MHz, d$_6$-DMSO, δ): 9.12–9.05 (s, 1H), 8.14–8.06 (m, 2H), 7.90–7.80 (m, 4H), 7.80–7.68 (m, 4H), 7.66–7.52 (m, 6H), 7.34–7.28 (m, 2H), 7.20–7.08 (m, 4H), 4.20 (t, 2H), 4.10 (t, 2H), 3.80 (s, 3H), 1.95–1.75 (m, 4H), 1.60–1.30 (m, 4H).

2.6. Synthesis of PPzP

Using a similar synthetic procedure of NPzN, compound PPzP was obtained by changing compound 3 instead of compound 2. Yield: 83%. ^{1}H NMR (300 MHz, d$_6$-DMSO, δ): 9.12–9.05 (s, 1H), 8.00–8.82 (m, 4H), 8.10–7.95 (m, 6H), 7.70–7.60 (m, 10H), 7.45–7.35 (m, 4H), 7.25–7.20 (m, 2H), 4.23 (t, 2H), 4.12 (t, 2H), 3.81 (s, 3H), 1.98–1.70 (m, 4H), 1.68–1.26 (m, 4H).

## 2.7. LEC device fabrication and characterization

Indium tin oxide (ITO) coated glass substrates were cleaned in ultrasonic bath of acetone, ethanol and isopropyl alcohol, dried in oven at 120 °C. After drying, PEDOT:PSS (poly(3,4-ethylenedioxythiophene)-poly(styrene sulfonate)) layer was spin-coated onto the ITO anode as a buffer layer and then dried in a vacuum over 120 °C for an hour. Then the active layer was spin-coated on top of PEDOT/PSS layer, 2 wt% solution in acetonitrile solution followed by annealing at 80 °C for 1 h in vacuum. Sequentially aluminum cathode contacts were deposited by thermal evaporation at high vacuum through a shadow mask on top of the active layer. Constant voltage scan was subjected to evaluate our device properties. Electroluminescence spectra and CIE color coordinates were measured using an Avantes luminance spectrum. The current density and luminance *versus* voltage characteristics were measured by using Keithley 2400 source meter coupled with an OPC 2100 optical spectrum analyzer.

3. Results and discussion

3.1. Thermal and photophysical properties

Thermal decomposition temperatures (T_d) and glass transition temperatures (T_g) of compounds were evaluated by using thermal gravimetric analysis (TGA) and differential scanning colorimetry (DSC) experiments. Both the compounds show high T_g of 102 and 118 °C for compounds NPzN and PPzP respectively. The thermal decomposition temperatures (T_d) (corresponding to 5% weight loss) of 383 and 303 °C for NPzN and PPzP were shown in Figs. S1 and S3. Photophysical characteristics of compounds were measured in dilute toluene solutions by using Ultraviolet-Visible (UUV–vis and photoluminescence (PL) spectrometers (Figs. 1 and 2).

NPzN shows maximum absorbance at 300 nm could be assigned to the π–π* transition of the molecular backbone. The compound was
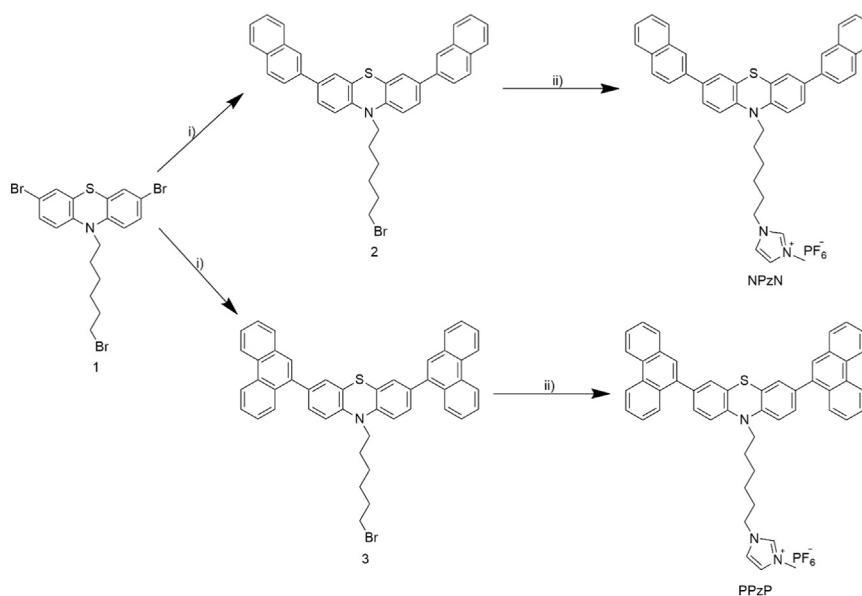
Scheme 1. i) Boronic acids, Pd(PPh$_3$)$_4$, K$_2$CO$_3$, TBAB, THF/water, ii) 1-methylimidazole, Toluene.
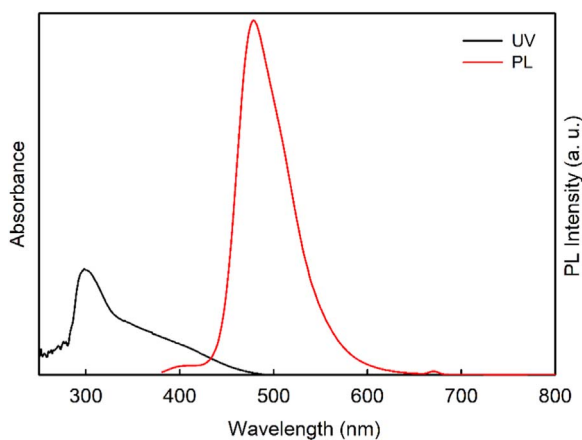

Fig. 1. Absorbance and photoluminescence spectra of compound NPzN in toluene solution.
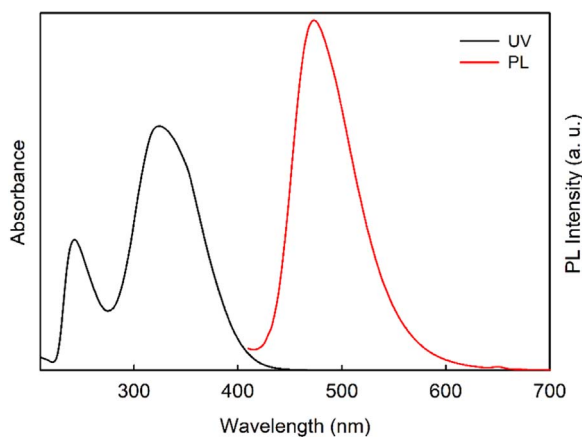

Fig. 2. Absorbance and photoluminescence spectra of compound PPzP in toluene solution.

exhibited maximum emission at 479 nm in dilute solution. Compound PPzP shows absorption maximum at 350 nm which is the characteristic π–π* transition of the compound. Photoluminescence spectra of compound PPzP shows peak at 473 nm which is sky-blue region. The energy

gap (E_g) of the compounds were evaluated from absorption spectrum was estimated to be 3.03 and 2.95 eV.

Photoluminescence quantum yield of the compound were measured to be 0.12 and 0.18 for NPzN and PPzP, respectively in toluene solution using 9,10-diphenylanthracene as a standard (Φ_f = 0.90 in cyclohexane). Thin-film PL spectra of both compounds (Fig. 3) were measured and the maximum emission were centered at 487 and 485 nm for NPzN and PPzP, respectively. All the physical data's were summarized in Table 1.

Thin-film emission of the compounds were slightly red-shifted compared solution emission spectra of the compounds due the intermolecular interactions in the solid-state of the compounds. Transient photoluminescence (Fig. S5) were measure in oxygen free toluene solution and the life time of the compounds were found to be 1.10 and 1.04 ns for compound NPzN and PPzP, respectively. measThe solvatochromic behaviors of both the compounds were examined in different solvents with different polarities. The compounds NPzN and PPzP exhibited positive solvatochromism upon increasing the polarity of the solvents (Figs. S6 and S7), showing the intramolecular charge transfer in the excited state. The results show positive solvatochromism with red-shifted emissions upon increasing the polarity of the solvent, which shows the sensitivity of the compounds to the solvent's polarity. These results suggest that the molecules NPzN and PPzP are beneficial green emitting materials in single-component electroluminescent devices.
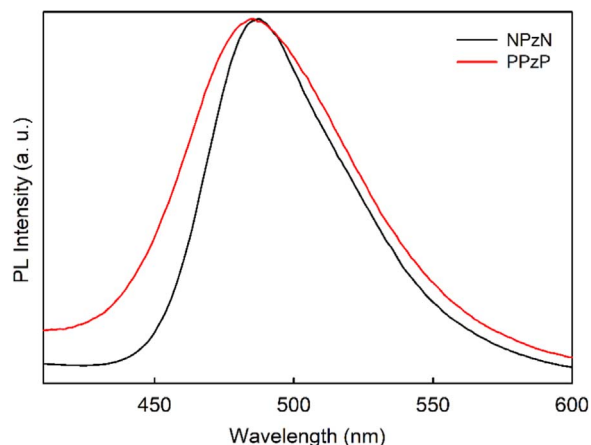

Fig. 3. Thin-film photoluminescence spectra of compound NPzN and PPzP.

Table 1
Photophysical and thermal properties.

Compounds	$\lambda_{UV,max}$[a] (nm)	$\lambda_{PL,max}$[b] (nm)	$\lambda_{PL,max}$[c] (nm)	Φ_f[d]	E_g[e] (eV)	T_d[f] (°C)
NPzN	300	479	487	0.12/0.02	3.03	383
PPzP	350	473	485	0.18/0.03	2.95	303

[a] Absorption in DCM (10^{-5} M).

[b] Photoluminescence in toluene (10^{-5} M).

[c] Thin-film photoluminescence.

[d] Photoluminescence quantum yield (PLQY) in toluene and thin film measured against DPA as standard.

[e] Optical band gap calculated from onset of absorption spectrum.
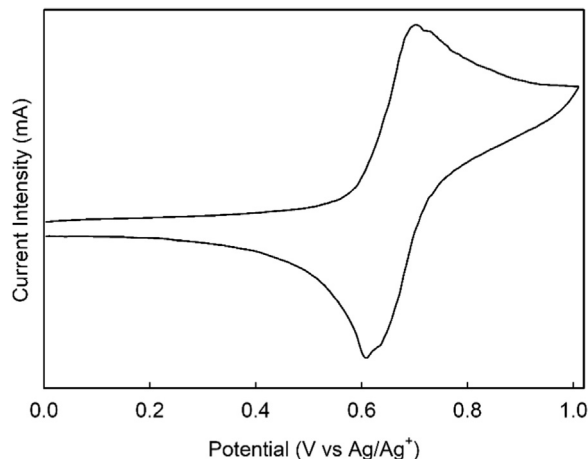
[f] Thermal decomposition (T_d) temperature.

Fig. 4. Cyclic voltammogram of NPzN.

3.2. Electrochemical properties

Electrochemical behaviors of NPzN and PPzP were investigated by cyclic voltammetry to measure the highest occupied molecular orbital (HOMO) levels of the compounds. The oxidation potential of the compounds was measured in acetonitrile solution containing t-butyl ammonium hexafluoro phosphate as supporting electrolyte shown in Figs. 4 and 5.

The HOMO energy level of both the compounds were estimated from the onset of oxidation curves and it was found to be − 5.03 and − 5.04 eV respectively for compounds NPzN and PPzP. The HOMO level of compounds suggests that it has good hole-injection ability due to strong electron donating ability of phenothiazine [57,58].
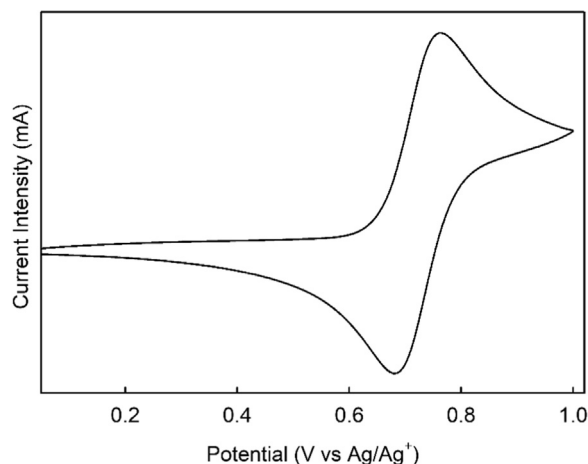

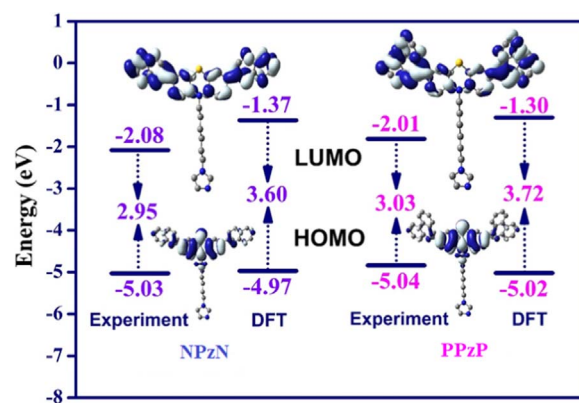**Fig. 5.** Cyclic voltammogram of PPzP.

Fig. 6. Electron density distribution in the frontier molecular orbitals of NPzN and PPzP.

Reduction potential was not observed for both the compounds during negative scanning. Therefore, the lowest unoccupied molecular orbital (LUMO) energy levels were calculated by adding the HOMO and the energy gaps (E_g) determined from their absorption edges UUV–visble spectrum. The estimated LUMO level was found to be − 2.00 and − 2.09 eV.

3.3. Theoretical calculations

The optimized geometry of the two compounds have been depicted in Figs. S8 and S9. The phenothiazine part of the molecules has a butterfly shape. The calculated bond angles in phenothiazine at Sulphur (*ca.* 99.5°) and Nitrogen (*ca.* 121.7°) are almost similar for the two compounds, which are in good agreement with the previously reported results [48,59]. The two rings (naphthalene in case of NPzN and phenanthrene in case of PPzP) attached to the central phenothiazine are not in the same plane with the phenothiazine.

The electron density distribution in HOMO and LUMO of the two compounds are shown in Fig. 6, in the same figure the eigenvalues of the frontier molecular orbitals have been given. The experimentally obtained electrochemical data from cyclic voltammetry is also given in the figure for comparison. The electron density in HOMO is localized over phenothiazine ring. While in the case of LUMO, the electron density has been spread over phenothiazine and attached two naphthalene/phenanthrene rings. The calculated eigenvalues of the HOMO are − 4.97 and − 5.02 eV for compound 1 and 2, respectively. The calculated eigenvalues of the LUMO are − 1.37 and − 1.30 eV for compound 1 and 2, respectively. The simulated electrochemical data are in good agreement with the corresponding experimental values. A small increase (0.08 eV) in the bandgap is observed from compound NPzN to compound PPzP which is also reproduced in simulations. The bandgap is increased by 0.12 eV from 3.60 eV to 3.72 eV for compound NPzN to compound PPzP. Experimental UUV–visble absorption spectra of the two compounds have been reproduced with the TDDFT methodology. To mimic the experimental condition (using toluene) in to obtain the UUV–visble spectra of the compounds, we simulated the spectra in the same solution using implicit PCM model. The UUV–visble absorption data obtained from the TDDFT simulations were given in Table S1 and the absorption spectra were depicted in Figs. S10 and S11. From the figure, the TDDFT simulations reproduced the main bands that were observed in the experimental spectrum. The simulated low energy absorption peak is observed at 339 and 326 nm for compounds NPzN and PPzP, respectively. The low energy intense absorption is occurring mainly due to the transitions from HOMO to LUMO for both compounds.

3.4. Electroluminescence properties

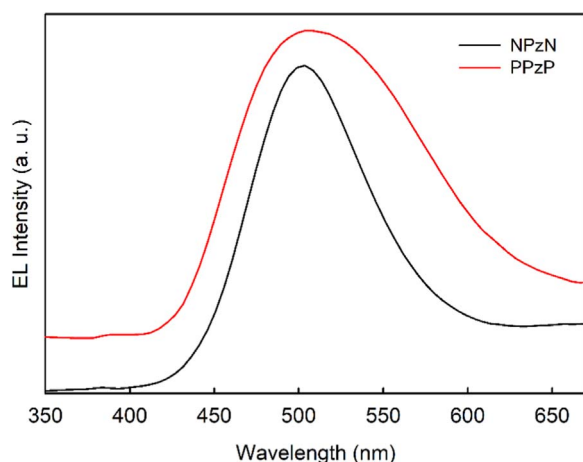The EL performance of NPzN and PPzP were investigated from

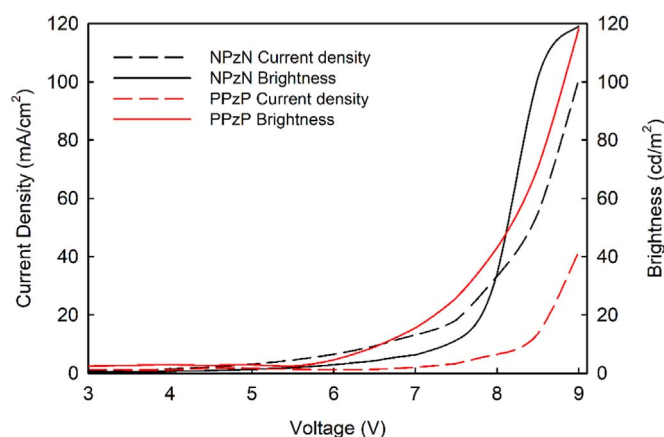Fig. 7. Electroluminescence spectrum of NPzN and PPzP.

Fig. 8. *J-V-L* curves of NPzN and PPzP.

single-component single-layered LECs devices. The devices were fabricated with configuration of ITO/PEDOT: PSS/Active layer/Al, in which ITO and Al were used as anode and cathode, respectively.

Active layer of the devices was spin coated from acetonitrile solution under ambient conditions.

LEC device performances were determined from Keithley 2400 source meter. LEC devices of compound NPzN exhibits electroluminescence centered at 499 nm with the CIE coordinates of (0.28, 0.43) was shown in Fig. 7. EL maximum centered at 505 nm was observed for compound PPzP with CIE coordinates of (0.32, 0.41). Both the devices exhibited red-shifted electroluminescence compared to their thin-film PL spectra due to the presence of intermolecular interaction of the molecules.

The exhibited EL of both the compounds were shifted to blue region compared with the previous phenothiazine based LEC report [48]. This is because of the presence of reduced intermolecular interaction of the compounds comparing with the previous sulfide derivative LECs. So that, improved CIE coordinates were observed for both the compounds. LEC devices shows green light-emission which is interested in constructing white light-emitting devices by blending of red-green-blue emitters in light-emitting devices [60]. The time-independent brightness (*L–V*) and current density (*J–V*) of the LEC devices were investigated by voltage scanning with sweep rate of 0.5 V/s. The *J-V-L* plots of the devices were depicted in Fig. 8. The maximum current density and brightness of 100 mA/cm^2 and 129 cd/m^2 was obtained for compound NPzN and current density and brightness of 42 mA/cm^2 and 59 cd/m^2 was observed for compound PPzP at 9.0 V in a solution processed LEC device. The performance produced by these compounds were lower as compared with the previous works due to the stability

and life time of the compounds [30,48]. However, the observed results are desirable for the fabrication of single component LEC devices.

4. Conclusions

We have designed and synthesized new green light-emitting molecules NPzN and PPzP containing electron donating phenothiazine as a central core. The synthesized compounds show blue-green emission in solution as well as in thin-films. Both the compounds exhibited good thermal stabilities. The intrinsic ionic nature of the compounds was utilized to fabricate single-layered electroluminescence devices. Both the devices show green light emission centered at 499 and 505 nm with CIE coordinates of (0.28, 0.43) and (0.32, 0.41) for compounds NPzN and PPzP, respectively. The absence of n-doping affects the performance of LEC devices and shows low brightness of 129 and 59 cd/m^2 respectively, for compounds NPzN and PPzP. These results suggest that the incorporation of aryl groups on phenothiazine has great effect on the optoelectronic properties of the materials.

Supporting information

TGA and DSC curves of NPzN and PPzP; Transient PL spectrum of NPzN and PPzP in an oxygen-free toluene solution; PL spectrum in different solvents of NPzN and PPzP; The DFT optimized ground state geometry of both the compounds.

Acknowledgements

Appendix A. Supplementary material

Supplementary data associated with this article can be found in the online version at http://dx.doi.org/10.1016/j.jlumin.2018.02.008.

References

[1] C.W. Tang, S.A. VanSlyke, Appl. Phys. Lett. 51 (1987) 913.
[2] Q.B. Pei, G. Yu, C. Zhang, Y. Yang, A.J. Heeger, Science 269 (1995) 1086.
[3] S. Daumann, D. Andrzejewski, M. Di Marcantonio, U. Hagemann, S. Wepfer, F. Vollkommer, G. Bacher, M. Epple, E. Nannen, J. Mater. Chem. C 5 (2017) 2344.
[4] B.M.D. Puscher, M.F. Ayguler, P. Docampo, R.D. Costa, Adv. Energy Mater. 7 (2017) 1602283.
[5] C. Larsen, R. Forchheimer, L. Edman, D. Tu, Org. Electron. 45 (2017) 57.
[6] J.E. Namanga, N. Gerlitzki, A.V. Mudring, Adv. Funct. Mater. 27 (2017) 1605588.
[7] E. Fresta, R.D. Costa, J. Mater. Chem. C 5 (2017) 5643.
[8] J. Zimmermann, L. Porcarelli, T. Rodlmeier, A.S. Sanchez, D. Mecerreyes, G.H. Sosa, Adv. Funct. Mater. (2018) 1705795.
[9] S. Tang, A. Sandstrom, P. Lundberg, T. Lanz, C. Larsen, S. Reenen, M. Kemerink, L. Edman, Nat. Commun. 8 (2017) 1190.
[10] J. Mindemark, L. Edman, J. Mater. Chem. C 4 (2016) 420.
[11] S. Tang, H.A. Buchholz, L. Edman, Appl. Mater. Interfaces 7 (2015) 25955.
[12] Q.B. Pei, Y. Yang, G. Yu, C. Zhang, A.J. Heeger, J. Am. Chem. Soc. 118 (1996) 3922.
[13] G. Hernandez-Sosa, R. Eckstein, S. Tekoglu, T. Becker, F. Mathies, U. Lemmer, N. Mechau, Org. Electron. 14 (2013) 2223.
[14] M.J. Jafari, J. Liu, I. Engquist, T. Ederth, ACS Appl. Mater. Interfaces 9 (2017) 2747.
[15] S. Tang, P. Murto, X. Xu, C. Larsen, E. Wang, L. Edman, Chem. Mater. 29 (2017) 7750.
[16] Y. Nishikitani, K. Suga, S. Uchida, S. Nishimura, K. Oyaizu, H. Nishide, Org. Electron. 51 (2017) 168.
[17] K.J. Chee, V. Kumar, C.V. Nguyen, J. Wang, P.S. Lee, J. Phys. Chem. C 120 (2016) 11324.
[18] R.D. Costa, E. Orti, H.J. Bolink, F. Monti, G. Accorsi, N. Armaroli, Angew. Chem. Int. Ed. 51 (2012) 8178.
[19] C.H. Lyons, E.D. Abbas, J.K. Lee, M.F. Rubner, J. Am. Chem. Soc. 120 (1998) 12100.
[20] E.S. Handy, A.J. Pal, M.F. Rubner, J. Am. Chem. Soc. 121 (1999) 3525.
[21] I. Gonzalez, P. Dreyse, D. Cortes-Arriagada, M. Sundararajan, C. Morgado, I. Brito, C. Rolda´n-Carmona, H.J. Bolink, B. Loeb, Dalton Trans. 44 (2015) 14771.
[22] C.D. Sunesh, G. Mathai, Y. Choe, Org. Electron. 15 (2014) 667.

[23] C.D. Sunesh, K. Shanmugasundaram, M.S. Subeesh, R.K. Chitumalla, J. Jang, Y. Choe, ACS Appl. Mater. Interfaces 7 (2015) 7741.

[24] C.-H. Yang, M. Mauro, F. Polo, S. Watanabe, I. Muenster, R. Fröhlich, L. De Cola, Chem. Mater. 24 (2012) 3684.

[25] L. He, J. Qiao, L. Duan, G.F. Dong, D.Q. Zhang, L.D. Wang, Y. Qiu, Adv. Funct. Mater. 19 (2009) 2950.

[26] T. Hu, L. He, L. Duan, Y. Qiu, J. Mater. Chem. 22 (2012) 4206.

[27] C.D. Sunesh, G. Mathai, Y. Choe, ACS Appl. Mater. Interfaces 6 (2014) 17416.

[28] Z.B. Hill, D.B. Rodovsky, J.M. Legera, G.P. Bartholomew, Chem. Commun. (2008) 6594.

[29] H.-F. Chen, C.-T. Liao, T.-C. Chen, H.-C. Su, K.-T. Wong, T.-F. Guo, J. Mater. Chem. 21 (2011) 4175.

[30] M.S. Subeesh, K. Shanmugasundaram, C.D. Sunesh, Y.S. Won, Y. Choe, J. Mater. Chem. C 3 (2015) 4683.

[31] S. Tang, W.Y. Tan, X.H. Zhu, L. Edman, Chem. Commun. 49 (2013) 4926.

[32] E. Fresta, G. Volpi, C. Garino, C. Barolo, R.D. Costa, Polyhedron 140 (2018) 129.

[33] A.K. Pal, A.F. Henwood, D.B. Cordes, A.M.Z. Slawin, I.D.W. Samuel, E.Z. Colman, Inorg. Chem. 56 (2017) 7533.

[34] P. Lundberg, E.M. Lindh, S. Tang, L. Edman, ACS Appl. Mater. Interfaces 9 (2017) 28810.

[35] M.D. Weber, M. Adam, R.R. Tykwinski, R.D. Costa, Adv. Funct. Mater. 25 (2015) 5066.

[36] M.D. Weber, J.E. Wittmann, A. Burger, O.B. Malcioglu, J.S. Marti, A. Hirsch, P.B. Coto, M. Bockstedte, R.D. Costa, Adv. Funct. Mater. 26 (2016) 6737.

[37] K.T. Weber, K. Karikis, M.D. Weber, P.B. Coto, A. Charisiadis, D. Charitaki, G. Charalambidis, P. Angaridis, A.G. Goutsolelos, R.D. Costa, Dalton Trans. 45 (2016) 13284.

[38] M.D. Weber, V. Nikolaou, J.E. Wittmann, A. Nikolaou, P.A. Angaridis, G. Charalambidis, C. Stangel, A. Kahnt, A.G. Coutsolelos, R.D. Costa, Chem. Commun. 52 (2016) 1602.

[39] A. Charisiadis, A. Bagaki, E. Fresta, K.T. Weber, G. Charalambidis, C. Stangel, A.G. Hatzidimitriou, P.A. Angaridis, A.G. Coutsolelos, R.D. Costa, ChemPlusChem 82 (2017) 1.

[40] H.-F. Chen, C.-T. Liao, M.-C. Kuo, Y.-S. Yeh, H.-C. Su, K.-T. Wong, Org. Electron. 13 (2012) 1765.

[41] A. Pertegas, D. Tordera, J.J. Serrano-Pérez, E. Ortí, H.J. Bolink, J. Am. Chem. Soc. 135 (2013) 18008.

[42] A. Pertegas, N.M. Shavaleev, D. Tordera, E. Ortí, M.K. Nazeeruddin, H.J. Bolink, J. Mater. Chem. C 2 (2014) 1605.

[43] M.Y. Wong, G.J. Hedley, G. Xie, L.S. Kölln, I.D.W. Samuel, A. Pertegás, H.J. Bolink, E. Zysman-Colman, Chem. Mater. 27 (2015) 6535.

[44] K. Shanmugasundaram, M.S. Subeesh, C.D. Sunesh, R.K. Chitumalla, J. Jang, Y. Choe, Org. Electron. 24 (2015) 297.

[45] M.S. Subeesh, K. Shanmugasundaram, C.D. Sunesh, T.P. Nguyen, Y. Choe, J. Phys. Chem. C 119 (2015) 23676.

[46] K. Shanmugasundaram, M.S. Subeesh, C.D. Sunesh, Y. Choe, RSC Adv. 6 (2016) 28912.

[47] M.S. Subeesh, K. Shanmugasundaram, C.D. Sunesh, R.K. Chitumalla, J. Jang, Y. Choe, J. Phys. Chem. C 120 (2016) 12207.

[48] M.S. Shanmugasundaram, C.D. Subeesh, R.K. Sunesh, J. Chitumalla, Y. Jang, J. Choe, Phys. Chem. C 120 (2016) 20247.

[49] M.S. Subeesh, T.P. Nguyen, Y. Choe, J. Phys. Chem. C 121 (2017) 14811.

[50] K. Shanmugasundaram, R.K. Chitumalla, J. Jang, Y. Choe, New J. Chem. 41 (2017) 9668.

[51] A.D. Becke, J. Chem. Phys. 98 (1993) 5648.

[52] A.D. Becke, J. Chem. Phys. 104 (1996) 1040.

[53] C. Lee, W. Yang, R.G. Parr, Phys. Rev. B 37 (1988) 785.

[54] T. Yanai, D.P. Tew, N.C. Handy, Chem. Phys. Lett. 393 (2004) 51.

[55] S. Miertus, E. Scrocco, J. Tomasi, J. Chem. Phys. 55 (1981) 117.

[56] M. Cossi, V. Barone, R. Cammi, J. Tomasi, Chem. Phys. Lett. 255 (1996) 327.

[57] S.A. Jenekhe, L. Lu, M.M. Alam, Macromolecules 34 (2001) 7315.

[58] A.P. Kulkarni, X. Kong, S.A. Jenekhe, Adv. Funct. Mater. 16 (2006) 1057.

[59] L. Yao, S. Sun, S. Xue, S. Zhang, X. Wu, H. Zhang, Y. Pan, C. Gu, F. Li, Y. Ma, J. Phys. Chem. C 117 (2013) 14189.

[60] T. Akatsuka, C. Roldan-Carmona, E. Orti, H.J. Bolink, Adv. Mater. 26 (2014) 770.